physica **p s s** status solidi **c**

www.pss-c.com

current topics in solid state physics

Ground State of Electron-Hole Bilayer
Kazuo Yamashita, Kenichi Asano,
Takuma Ohashi

physica **p s s** status solidi **b**

www.pss-b.com

basic solid state physics

New article series

Advanced Calculations
for Defects in Materials –
Electronic Structure
Methods

Feature Article

Chris G. Van de Walle
and Anderson Janotti

physica **p s s** status solidi **a**

www.pss-a.com

applications and materials science

Expert Opinion
Solid-state lighting
Roland Haitz and Jeffrey Y. Tsao

WILEY-VCH

physica **p s s** status solidi **rrl**

www.pss-rapid.com

rapid research letters

New: review@rrl

Competing energy scales in
high-temperature superconductors:
Ultrafast pump-probe studies
Elbert E. M. Chia, Jian-Xin Zhu,
D. Talbayev, and A. J. Taylor

WILEY-VCH

WILEY-VCH

Light scattering by a metallic nanoparticle coated with a nematic liquid crystal

Vassilios Yannopapas*, Nikolaos Fytas, Vicky Kyrimi, Efthymios Kallos, Alexandros G. Vanakaras, and Demetri J. Photinos

Department of Materials Science, University of Patras, 26504 Patras, Greece

* Corresponding author: e-mail vyannop@upatras.gr, Phone: +30-2610-969382, Fax: +30-2610-969368

We study the optical properties of gold nanoparticles (NPs) coated with a nematic liquid crystal (NLC) whose director field is distributed around the NP according to the anchoring conditions at the surface of the NP. The distribution of the NLC is obtained by minimization of the corresponding Frank free-energy functional whilst the optical response is calculated by the discrete-dipole approximation (DDA). We find, in particular, that the anisotropy of the NLC coating does not affect much the (isotropic) optical response of the NP. However, for strong anchoring of the NLC molecules on the surface of NP, the inhomogeneity of the coating which is manifested by a ring-type singularity (disclination or Saturn ring), produces an enhancement of the extinction cross spectrum over the entire visible spectrum.

1 Introduction Metamaterials are man-made structures with electromagnetic (EM) properties which are not met in naturally occurring materials, such as artificial magnetism, negative refractive index (NRI), near-field amplification, cloaking, and other optical illusions. The holy grail of research in this discipline has been the realization of metamaterials with the above EM properties in the visible regime. To this end, top-down technologies and lithographic techniques have been employed for the realization of optical metamaterials. However, due to fabrication restrictions in the top-down approaches, only two-dimensional (2D), planar metamaterials have been realized in the optical regime [1]. On the contrary, bottom-up approaches based on self-assembly technology allow for the realization of true, three-dimensional (3D) optical metamaterials with the promise of lower cost, high throughput, and small sensitivity to damage or fabrication errors.

The most promising way of realizing metamaterials by a bottom-up approach relies on organic chemistry of mesogens and macromolecules. Namely, macromolecules such as dendrimers and mesogens of controlled shape are ideally suited for organizing metal nanoparticles (NPs) into composite materials with tailored properties such as particle size, shape, particle distance, etc. Macromolecular and low-molar liquid crystal (LC) ligands are attached to the particles by chemical methods and arrangements such as disks or rods can be envisaged where the NP is located at the center and is surrounded by radially or tangentially arranged organic molecules [2–7].

In this work, we study the optical response of a single metallic NP decorated by a nematic liquid crystal (NLC), in order to assess the effect of the inherent inhomogeneity and anisotropy of the NLC on the plasmonic excitation of the metallic NP. Our study will be based on treating the NLC surrounding the NP as a continuous medium but with the aforementioned inhomogeneity and anisotropy of the NLC. The anisotropy of the NLC stems from the axial symmetry of NLC molecules whilst the inhomogeneity is a result of the anchoring of the NLC molecules on the surface of the NP. The distribution of the director field of the NLC around a certain NP is taken by minimization of the corresponding functional of the elastic Frank free energy around and at the surface of the NP. For two limiting cases for the anchoring energy, i.e., $W \to 0$ (weak anchoring) and $W \to \infty$ (strong anchoring) we use analytic expressions for the spatial distribution of the director field. A spherical metallic NP is assumed to be coated by a spherical layer of an NLC with given director-field distribution. The EM response of the

NLC-coated NP is studied by means of the discrete-dipole approximation (DDA) [8–10] using as input the polarizability tensor at each point in space which is provided by the distribution of the director field for the NLC coating (the corresponding polarizability tensor for the metallic NP/core is diagonal and constant in space). It is worth noting that the optical response of NLC-coated metallic NP in free space [11] and atop a substrate [12] has been studied in the past within, however, a limited frequency range around the NP surface plasmon (SP) frequency.

2 Theory
2.1 Distribution of the director field
In the absence of any material boundaries, an NLC is uniformly distributed in space. However, when boundaries are present the director field of the NLC is inhomogeneously distributed in space according to the anchoring conditions on the physical boundary. In our case, the physical boundary is the surface of the NP. In order to find the distribution of the director field $\boldsymbol{n}(\boldsymbol{r})$ around the NP, one minimizes the functional of the Frank free energy which, in our case, is taken in the one-constant approximation, i.e.,

$$F = \int \frac{1}{2} K \left[(\nabla \cdot \boldsymbol{n})^2 + (\nabla \times \boldsymbol{n})^2 \right] \mathrm{d}^3 r. \qquad (1)$$

At the surface of NP, the functional of the free energy is taken in the Rapini and Popoular [13] approximation

$$F_s = -\oint \frac{1}{2} W(\boldsymbol{n} \cdot \hat{\boldsymbol{s}}) \mathrm{d}S, \qquad (2)$$

where $\hat{\boldsymbol{s}}$ is the unit vector normal to the surface and W the anchoring energy. Equation (2) constitutes the boundary condition in our case. The functionals of Eqs. (1) and (2) are minimized under the constraint $|\boldsymbol{n}(\boldsymbol{r})|^2 = 1$ for the director vector

$$\begin{aligned} \boldsymbol{n}(\boldsymbol{r}) &= (n_x, n_y, n_z) \\ &= (\sin\beta(\boldsymbol{r})\cos\phi, \ \sin\beta(\boldsymbol{r})\sin\phi, \ \cos\beta(\boldsymbol{r})), \end{aligned} \qquad (3)$$

which, obviously, respects the cylindrical symmetry of the problem (θ, ϕ are the polar and azimuthal angles of the spherical coordinate system). $\beta(\boldsymbol{r})$ is the angle between the director vector and the z-axis which is taken to be the optical axis of the NLC in the absence of the NP.

For the case of *weak* anchoring, i.e., $WS/K \ll 1$ where S is the NP radius, minimization of the functionals (1) and (2) leads to an analytical function for $\beta(\boldsymbol{r})$ [14]

$$\beta(\boldsymbol{r}) = \frac{WS}{4K} \left(\frac{S}{r} \right)^3 \sin 2\theta. \qquad (4)$$

The above formula is valid for anchoring energies $W \leq 10^{-4}\,\mathrm{erg\,cm^{-2}}$. For a typical value of $K \sim 10^{-6}\,\mathrm{erg\,cm^{-1}}$, Eq. (4) is valid for NP radii $S < 5\,\mu\mathrm{m}$ [14].

For the case of *strong* anchoring, i.e., $W \to \infty$, one can also have an analytic function for $\beta(\boldsymbol{r})$ [14]

$$\beta(\boldsymbol{r}) = \theta - \frac{1}{2}\arctan\left(\frac{\sin 2\theta}{1/f(r) + \cos 2\theta} \right), \qquad (5)$$

where

$$f(r) = \left(\frac{r}{a} \right)^3 + A + B + C\exp(-r/a), \qquad (6)$$

and

$$\begin{aligned} A = \frac{S^3}{a^2(a-S)^2} &\left[S - a + \left(\frac{a}{S} \right)^2 (4a - 3S) \right. \\ &\left. \times \left[\frac{a}{S}\exp(-S/a) - \exp(-1) \right] \right], \end{aligned}$$

$$\begin{aligned} B = \frac{S^3}{a^2(a-S)^2} &[a - S + (4a - 3s) \\ &\times [\exp(-1) - \exp(-S/a)]], \end{aligned}$$

$$C = -\frac{4a - 3S}{a - S}. \qquad (7)$$

$r = a$ is the distance from the center of the NP of a disclination (Saturn) ring of $(-1/2)$ singularity at the equatorial plane ($\theta = \pi/2$) [14–16]. The Saturn ring is a result of the pinning of the NLC to the surface of the NP. We note that the above analytical functions for the NLC director field are valid for two limiting cases (weak and strong anchoring). For intermediate anchoring energies as well as for more general Frank free-energy functionals one has to resort to numerical methods [11, 12, 17–21].

2.2 Discrete-dipole approximation
We study the optical response of NLC-coated metallic NP using the DDA [8–10]. The NLC-coated NP (scattering object in our case) is considered as an array of point dipoles ($i = 1, \cdots, N$) each of which is located at the position $\boldsymbol{r}_i$, corresponding to a dipole moment $\boldsymbol{P}_i$ and a (position-dependent) polarizability tensor $\tilde{\alpha}_i$. The above quantities are connected by

$$\boldsymbol{P}_i = \tilde{\alpha}_i \boldsymbol{E}_i, \qquad (8)$$

where $\boldsymbol{E}_i$ is the electric field at i-th dipole,

$$\boldsymbol{E}_i = \boldsymbol{E}_{\mathrm{inc},i} - \sum_{j \neq i} \boldsymbol{A}_{ij} \cdot \boldsymbol{P}_j, \qquad (9)$$

which is the sum of the directly incident field $\boldsymbol{E}_{\mathrm{inc},i}$ as well as the field scattered by all the other dipoles $j \neq i$ and it is incident on the i-th dipole [second term of Eq. (9)]. The

interaction matrix A_{ij} is given from

$$A_{ij} = \frac{\exp(ikr_{ij})}{r_{ij}} \left[k^2 (\hat{r}_{ij}\hat{r}_{ij} - 1_3) \right.$$
$$\left. + \frac{ikr_{ij} - 1}{r_{ij}^2} (3\hat{r}_{ij}\hat{r}_{ij} - 1_3) \right], \quad i \neq j, \quad (10)$$

where 1_3 is the 3×3 unit matrix, $r_{ij} = r_i - r_j$, $\hat{r}_{ij} = r_{ij}/|r_{ij}|$. By combining Eqs. (8) to (10) we obtain a linear system of equations, *i.e.*,

$$\sum_{j=1}^{N} A_{ij}P_j = E_{\text{inc},i}, \quad (11)$$

where the diagonal elements of the interaction matrix are essentially the inverse of the polarizability tensor of each dipole, *i.e.*,

$$A_{ii} = [\tilde{\alpha}_i]^{-1}. \quad (12)$$

For an anisotropic sphere characterized by a dielectric tensor $\tilde{\varepsilon}_s$ and immersed within an isotropic host of dielectric constant ε_h, the polarizability tensor of the sphere is given by the Clausius–Mossoti formula for anisotropic spheres [22], *i.e.*,

$$\tilde{\alpha}_i = V_s \frac{3\varepsilon_h}{4\pi} [\tilde{\varepsilon}_s - \varepsilon_h 1_3][\tilde{\varepsilon}_s + 2\varepsilon_h 1_3]^{-1}. \quad (13)$$

For an NLC $\tilde{\varepsilon}_s = \text{diag}(\varepsilon_\parallel, \varepsilon_\parallel, \varepsilon_\perp)$ while for a metallic sphere $\tilde{\varepsilon}_s = \varepsilon_m 1_3$. Eq. (13) provides the polarizability of an NLC when the director vector is oriented along the z-axis of the (global) coordinate system. When the director vector of the i-th dipole forms arbitrary angles α, β, and γ with the x, y, and z axes, respectively, the polarizability tensor is given by [23]

$$\hat{\alpha} = M^{-1}\tilde{\alpha}M, \quad (14)$$

where

$$M = R_x(\alpha)R_y(\beta)R_z(\gamma), \quad (15)$$

and $R_x(\alpha)$, $R_y(\beta)$, $R_z(\gamma)$ are the rotation matrices about the x, y, and z axes, respectively.

Having determined the dipole moment P_i at each point dipole, one can calculate quantities such as the scattering, extinction, and absorption cross-sections, *i.e.*,

$$C_{\text{sc}} = \frac{4\pi k}{|E_{\text{inc}}|^2} \sum_{i=1}^{N} \left[\frac{2}{3}k^2|P_i|^2 - \Im(P_i \cdot E_{\text{self},i}^*) \right], \quad (16)$$

$$C_{\text{ext}} = 4\pi k \sum_{i=1}^{N} \Im\left(P_i \cdot E_{\text{inc},i}^* \right), \quad (17)$$

$$C_{\text{abs}} = 4\pi k \sum_{i=1}^{N} \Im\left(P_i \cdot E_i^* \right), \quad (18)$$

where $E_{\text{self},i} = E_i - E_{\text{inc},i}$.

2.3 Nonlocal optical response for the gold nanoparticle Due to the small size (below 10 nm) of the fabricated NLC-coated gold NPs, the dielectric function of gold appearing in Eq. (13) should be provided within a nonlocal description of the optical response of a NP [24–29]. At the same time, a realistic description of the optical properties of NLC-coated NPs requires the adoption of an experimentally obtained dielectric function [30] which, apart from the Drude-type behavior, it includes the contribution of interband transitions. Lastly, due to the small size of the NP, scattering of the free electrons at the boundaries of the NP should be considered as well. Taking all the above into account, the dielectric function of gold is written [28],

$$\varepsilon_m(\omega, k) = \varepsilon_{\text{exp}}(\omega) - \varepsilon_{\text{Drude}}(\omega) + \varepsilon_{\text{NL}}(\omega, k), \quad (19)$$

where ε_{exp} is the experimental dielectric function of gold [30] and

$$\varepsilon_{\text{Drude}} = 1 - \frac{\omega_p^2}{\omega(\omega + i\gamma_{\text{bulk}})}, \quad (20)$$

is the Drude-type dielectric function where $\omega_p = 8.99$ eV and $\gamma_{\text{bulk}} = 0.05$ eV are the plasma frequency and the loss factor of bulk gold, respectively. The nonlocal part of the dielectric function of Eq. (19) is provided by the hydrodynamic model [24, 26, 29]

$$\varepsilon_{\text{NL}} = 1 - \frac{\omega_p^2}{\omega^2 + i\omega\gamma_{\text{NP}} - \beta k^2}, \quad (21)$$

where $\beta = (3/5)v_F^2$ with $v_F = 0.903$ eV nm being the electron Fermi velocity for gold. γ_{NP} is the loss factor (inverse relaxation time of the free electrons) corrected in order to take into account the scattering of the electrons at the spherical boundary of the NP [31]

$$\gamma_{\text{NP}} = \gamma_{\text{bulk}} + Gv_F/S, \quad (22)$$

where S is the NP radius and G is a dimensionless fitting parameter which describes the nature of the electron-surface scattering [31]. In Figs. 2–4 we have taken $G = 1$ whilst in Fig. 5 we have taken $G = 3$ for best fitting to the experimental data.

Once a nonlocal dielectric function is assumed for the gold NP, the corresponding polarizability must be given in the same (nonlocal) framework, *i.e.*, $\tilde{\alpha}_i$ of Eq. (13) is provided by [26, 28, 29]

$$\tilde{\alpha}_i = V_s \frac{3\varepsilon_h}{4\pi} \left[\tilde{\zeta}_s - \varepsilon_h 1_3 \right] \left[\tilde{\zeta}_s + 2\varepsilon_h 1_3 \right]^{-1}, \quad (23)$$

with

$$\tilde{\zeta}_s = \left[\frac{6S}{\pi} \int_0^\infty dk \frac{j_1^2(kS)}{\varepsilon_m(\omega, k)} \right]^{-1}, \quad (24)$$

where j_1 is the spherical Bessel function for $\ell = 1$ and ε_m is given by Eq. (19). Thanks to the homogeneous and isotropic nature of the NPs studied here as well as their small size

(<10 nm), a gold NP can be very well approximated as a *single* point dipole in Eq. (11) whose polarizability is provided by the nonlocal polarizability of Eq. (24). This speeds up the convergence in the DDA calculations [numerical solution of Eqs. (11)] since the gold NP need not be further discretized to smaller dipoles.

3 Results and discussion We consider gold NPs coated by E7 commercially available NLC with refractive indices $n_\parallel = 1.74$ and $n_\perp = 1.53$ [32]. Figure 1 shows a gold NP surrounded by a Saturn ring of $-1/2$ singularity which is present under strong anchoring conditions. Figure 2 shows the extinction spectrum for a gold NP of 7.5 nm radius surrounded by an NLC coating of 5 nm thickness for right-circularly polarized light incident along (Fig. 2a) and normal (Fig. 2b) to the NLC optical axis.

We note that the scattering spectrum is much smaller than the absorption spectrum, *i.e.*, extinction almost exclusively stems from absorption. The calculated extinction spectra are for weak ($WS/K = 2 \times 10^{-4}$) and strong anchoring conditions as well as for the case of an isotropic medium whose refractive index is the average of two refractive indices of the NLC, *i.e.*, $n_{\text{iso}} = (2n_\parallel + n_\perp)/3$.

Figure 3 shows extinction spectra similar to those of 2 but for a thicker coating, *i.e.*, 7.5 nm thickness. The peak in all extinction spectra stems from the excitation of the SP resonance of the gold NP. Evidently, for strong anchoring conditions, the extinction spectrum is on the average 20% higher than the two other types of coating (weakly anchored NLC and isotropic). Figure 4 shows the position of the SP peak as a function of the coating thickness, for different configurations of the NLC director field and different directions of light incidence. As the coating becomes thicker, the difference in the SP position between the isotropic LC and the NLC phases increases, *i.e.*, for a 7.5 nm thickness and for incidence along the NLC axis, the SP peak for weak anchoring conditions is 5 nm below the SP peak corresponding to the isotropic LC coating.

It can also be seen that the position of the SP depends on the incidence direction (and hence on polarization) as a result of the inherent anisotropy of the NLC coating which induces
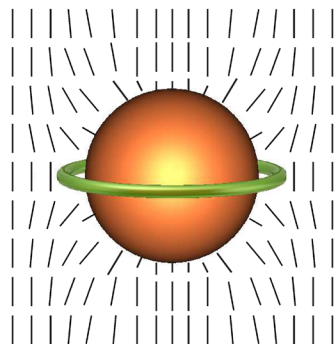

Figure 1 (online color at: www.pss-a.com) A metallic NP coated with a strongly anchored NLC and its disclination ring at the equatorial plane.
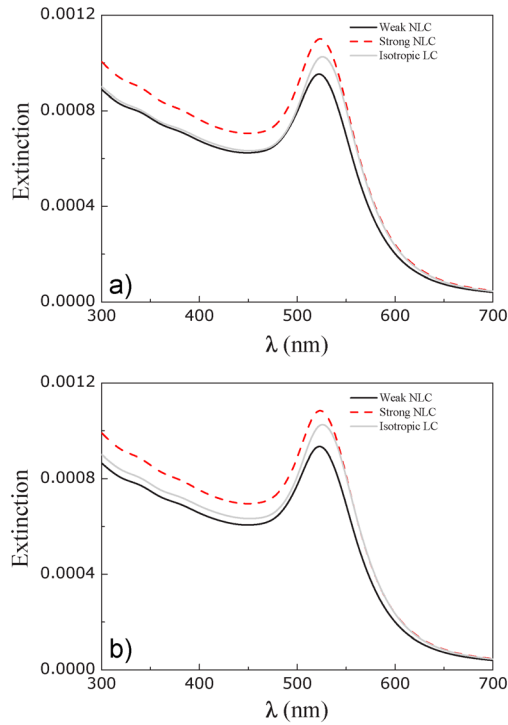

Figure 2 (online color at: www.pss-a.com) Extinction spectrum for a 7.5 nm gold NP coated with E7 NLC of 5 nm thickness for weak (solid line) and strong (broken line) anchoring conditions. The light gray line corresponds to the case of an isotropic medium with $n_{\text{iso}} = (2n_\parallel + n_\perp)/3$. For (a) light is incident along the optical axis of the NLC (taken to be the z-axis) while for (b) light is incident normal to the optical axis.

the splitting of the SP mode [11, 12]. The splitting is somewhat larger for the weak anchoring conditions implying a more anisotropic profile for the director-field distribution. As expected, the SP splitting is zero for the isotropic LC phase.

The small differences in the position (about 1 nm) and magnitude (about 2%) of the extinction spectra for both cases of incidence (parallel and normal to the optical axis of the NLC) indicates that the anisotropy of the NLC does not affect much the (isotropic) EM response of the NP. This means that in a periodic metamaterial structure made from NLC-functionalized metallic NPs, if anisotropic optical response is experimentally measured it must be mostly attributed to the particular arrangement of the NPs in space and very little to the anisotropy of the surrounding medium (NLC) which will only have the role of a "glue" which keeps the NPs joint together in a certain geometrical structure. Of course, as mentioned above, the inhomogeneous distribution of the NLC around the metallic NP should be taken into account as it results in an overall 20% higher extinction spectrum for strong anchoring conditions and a considerable SP shift of about 5 nm for weak anchoring conditions. We note, however, than neither the anisotropy nor the inhomogeneity of the NLC coating produces new structure, *e.g.*, additional
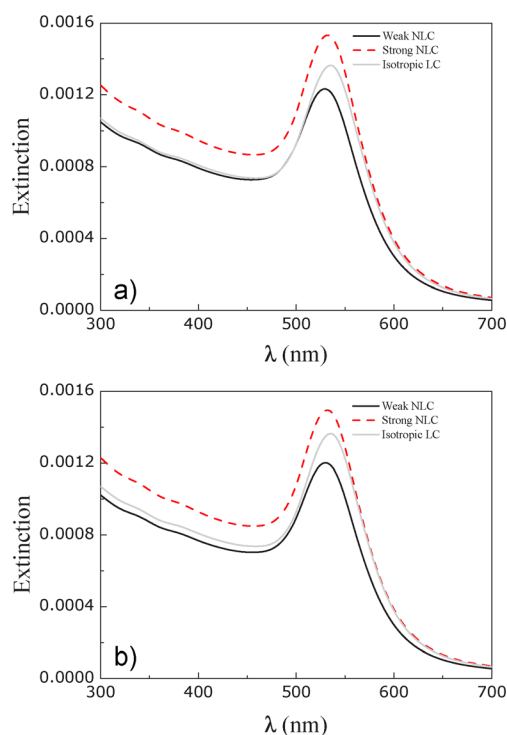
Figure 3 (online color at: www.pss-a.com) The same as Fig. 2 but for an NLC coating of 7.5 nm thickness.

peaks, in the extinction spectrum as a result of the small anisotropy of the refractive index.

Finally, in Fig. 5 we show the absorption spectrum for a gold NP in the NLC 4-cyano-4-n-pentylbiphenyl (5CB) along with corresponding experimental data from Ref. [4]. The agreement between theory and experiment is very good except for wavelengths shorter than 475 nm where the theoretical curve is a decreasing function of wavelength while the experimental one is increasing. It is worth noting that our theoretical model cannot capture experimental conditions such as the free rotation and the size distribution of the NPs.
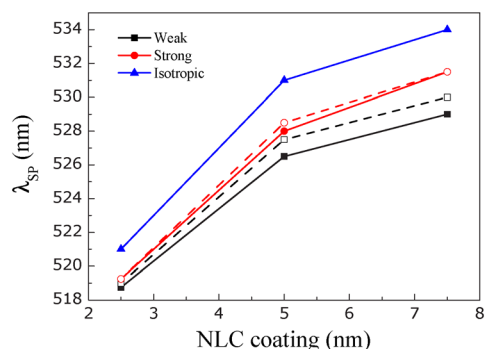

Figure 4 (online color at: www.pss-a.com) Position of the SP peak for different configurations of the NLC director field, for light incident along (solid lines – filled symbols) and normal (broken lines – empty symbols) to the optical axis of the NLC.
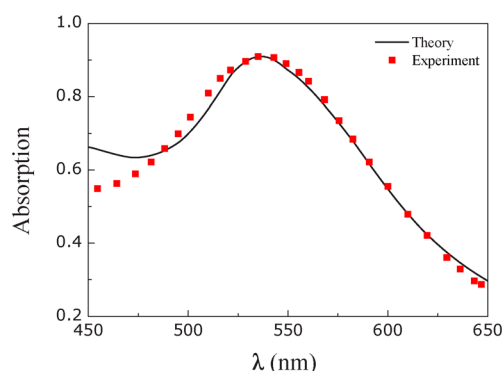

Figure 5 (online color at: www.pss-a.com) Theoretical (line) and experimental (squares) absorption spectra for a 6 nm gold NP within the NLC 4-cyano-4-n-pentylbiphenyl (5CB). The theoretical curve is taken by assuming $G = 3$ in Eq. (22).

4 Conclusions We have studied the optical response of gold NPs coated with an NLC. The distribution of the director field of the NLC was taken from analytic functions determined by minimization of the elastic Frank free energy. The optical response has been calculated by the DDA which takes into account both the anisotropy and inhomogeneity of the LC coating. We have found that the anisotropy of the coating has small influence on the (isotropic) response of the NP. If the LC molecules are strongly anchored at the surface of the NP, the distribution of the NLC possess a topological singularity (Saturn ring) and has a significant impact on the magnitude of the extinction spectrum of the NP. For weakly anchored LC molecules, the SP peak is shifted a few nm relative to a coating of isotropic LC phase.

References

[1] C. M. Soukoulis and M. Wegener, Nature Photon. **5**, 523 (2011).
[2] L. Cseh and G. H. Mehl, J. Am. Chem. Soc. **128**, 13376 (2006).
[3] X. Zeng, F. Liu, A. G. Fowler, G. Ungar, L. Cseh, G. H. Mehl, and J. E. Macdonald, Adv. Mater. **21**, 1746 (2009).
[4] S. Khatua, P. Manna, W.-S. Chang, A. Tcherniak, E. Friedlander, E. R. Zubarev, and S. Link, J. Phys. Chem. C **114**, 7251 (2010).
[5] Q. Liu, Y. Cui, D. Gardner, X. Li, S. He, and I. I. Smalyukh, Nano Lett. **10**, 1346 (2010).
[6] K. Kanie, M. Matsubara, X. Zeng, F. Liu, G. Ungar, H. Nakamura, and A. Muramatsu, J. Am. Chem. Soc. **134**, 808 (2011).
[7] C. H. Yu, C. P. J. Schubert, C. Welch, B. J. Tang, M.-G. Tamba, and G. H. Mehl, J. Am. Chem. Soc. **134**, 5076 (2012).
[8] E. M. Purcell and C. R. Pennypacker, Astrophys. J. **186**, 705 (1973).

 [9] P. J. Flatau, Opt. Lett. **22**, 1205 (1997).
[10] M. A. Yurkin and A. G. Hoekstra, J. Quantum Spectrosc. Radiat. Transfer **106**, 558 (2007).
[11] S. Y. Park and D. Stroud, Appl. Phys. Lett. **85**, 2920 (2004).
[12] S. Y. Park and D. Stroud, Phys. Rev. Lett. **94**, 217401 (2005).
[13] A. Rapini and M. Popoular, J. Phys. (Paris) Colloq. **30**, C-4-54 (1969).
[14] O. V. Kuksenok, R. W. Ruhwandl, S. V. Shiyanovskii, and E. M. Terentjev, Phys. Rev. E **54**, 5198 (1996).
[15] E. M. Terentjev, Phys. Rev. E **51**, 1330 (1995).
[16] T. C. Lubensky, D. Pettey, N. Currier, and H. Stark, Phys. Rev. E **57**, 610 (1998).
[17] R. W. Ruhwandl and E. M. Terentjev, Phys. Rev. E **56**, 5561 (1997).
[18] H. Stark, Eur. Phys. J. B **10**, 311 (1999).
[19] S. Grollau, N. L. Abbott, and J. J. de Pablo, Phys. Rev. E **67**, 011702 (2003).
[20] J. Fukuda, M. Yoneya, and H. Yokoyama, Eur. Phys. J. E **13**, 87 (2004).

[21] D. L. Cheung and M. P. Allen, Phys. Rev. E **74**, 021701 (2006).
[22] O. Levy and D. Stroud, Phys. Rev. B **56**, 8035 (1997).
[23] V. A. Loiko and V. I. Molochko, Appl. Opt. **38**, 2857 (1999).
[24] R. Ruppin, Phys. Rev. B **11**, 2871 (1975).
[25] G. S. Agarwal and S. V. O'Neil, Phys. Rev. B **28**, 487 (1983).
[26] R. Fuchs and F. Claro, Phys. Rev. B **35**, 3722 (1987).
[27] A. Liebsch, Phys. Rev. B **48**, 11317 (1993).
[28] F. J. García de Abajo, J. Phys. Chem. C **112**, 17983 (2008).
[29] C. W. Chen, L. S. Liao, H.-P. Chiang, and P. T. Leung, Appl. Phys. B **99**, 223 (2010).
[30] R. B. Johnson and R. W. Christy, Phys. Rev. B **6**, 4370 (1972).
[31] N. K. Grady, N. J. Halas, and P. Nordlander, Chem. Phys. Lett. **399**, 167 (2004).
[32] J. Li, Y. Ma, Y Y. Gu, I. C. Khoo, and Q. Gong, Appl. Phys. Lett. **98**, 213101 (2011).